AIMS Mathematics, 11(4): 9612–9632.
DOI: 10.3934/math.2026398
Received: 14 December 2025
Revised: 20 March 2026
Accepted: 31 March 2026
Published: 10 April 2026

https://www.aimspress.com/journal/Math

*Research article*

# Inverse protocol for determining the explosive mass of unstable substances in real accidental explosions

**Juan Francisco Sánchez-Pérez*, Manuel Conesa, José Jodar, Enrique Castro and Martina Fernández-García**

Department of Applied Physics and Naval Technology, Area of Applied Physics, Universidad Politécnica de Cartagena (UPCT), Cartagena, Spain

* **Correspondence:** Email: juanf.sanchez@upct.es.

**Abstract:** This paper presents an inverse problem protocol designed to estimate the explosive mass involved in accidental explosions by analyzing the observed effects on structures and individuals. Theoretical equations for calculating overpressure and momentum—which, although less accurate than finite element simulations, do not require significant computational resources—and the Probit methodology for damage quantification are widely employed. By applying both techniques, this study identifies the most suitable effects for applying the inverse problem, considering their distribution relative to distance and explosive mass. Mortality-related effects are considered unreliable due to their extremely narrow range, introducing significant uncertainty. However, eardrum rupture offers a broader distribution, although its practical application is complex due to the difficulties in determining both the distance to the population and the percentage of affected individuals. Conversely, structural damage to buildings proves to be the most accurate and reliable indicator, facilitated by GIS-based distance measurements and the clear categorization of damage levels. Finally, the use of a confidence interval in the inverse problem protocol allows for the filtering of highly biased data, ensuring that unreliable observations do not compromise the accuracy of the result. Furthermore, analysis demonstrates that a 90% confidence level minimizes relative error and improves robustness. In conclusion, a protocol is presented that allows the determination of the mass of the unstable substance involved in accidental explosions, specifying both the appropriate statistical indicators and the effects that are suitable for use in the inverse problem.

**Keywords:** inverse problem; statistics in engineering; accidental explosions; Probit methodology; simulation

**Mathematics Subject Classification:** 15A29, 76M21, 62P30, 62P35

## Nomenclature

| | |
|---|---|
| α | confidence level value |
| σ | standard deviation |
| ρ | density of the gas (kg/m$^3$) |
| $A$ | factor used to develop fundamental equations |
| a | empirical constant |
| b | empirical constant |
| F | factor used to develop fundamental equations |
| f | equivalence factor between an explosive and TNT |
| h | specific enthalpy (J/kg) |
| n | number of data |
| p | pressure (Pa) |
| r | actual distance from the center of the explosion (m) |
| R | ideal gas constant (J/mol·K) |
| T | absolute temperature (K) |
| u | velocity of the gas (m/s) |
| v | specific volume of the gas (m$^3$/kg) |
| W | mass of the explosive (kg) |
| $W_{TNT}$ | TNT equivalent mass (kg) |
| Y | Probit value (dimensionless) |
| z | scaled distance from the explosion's centrre (m/kg$^3$) |

**Subscripts** (for other subscripts not listed, see general nomenclature)

| | |
|---|---|
| 1,2 | refers to the gas entering and leaving the shock wave |

**Superscripts**

| | |
|---|---|
| i = I, II, III,… | refer to each iteration or simulation for the second stage |
| j = I, II, III,… | refer to each iteration or simulation for the first stage |

## 1. Introduction

An explosion is a very significant industrial hazard in terms of its damage potential, which can lead to fatalities and property damage. Some examples of its catastrophic consequences are the Beirut explosion accident in 2020, which resulted in 178 fatalities and more than 6500 injured people [1], the explosion of Ruihai International Logistics Co., Ltd. (Tianjin, China) [2], which caused 173 fatalities, 798 injured, people and a financial loss of almost USD 2 billion, and the explosion at Tianjiayi Chemical Co (Xiangshui County, Yancheng city, China) in 2019, which led to 78 fatalities, more than 617 injured people, and property losses of USD 100 million [3]. Explosion prevention is a duty for industries and workers in charge of explosive materials, who require all available tools and information to do it in the best possible way.

For adequate prevention, it is essential to use mathematical models that allow us to assess the consequences of any risk or situation, such as explosions. There are many processes that can be described using mathematical models that relate causes to effects. The main application of a

mathematical model is to predict the behavior of a system based on its initial state and boundary conditions. Predicting the response of the system based on known data is called a direct problem. If the model and data accurately describe a realistic physical situation, the direct problem is typically well-posed, meaning that the existence, uniqueness, and continuous dependence of the solution are guaranteed [4,5].

Solving the direct problem allows us to study the possible consequences of an explosion, being a useful tool for developing prevention plans that minimize catastrophic consequences. Many researchers have studied the consequences of different types of explosions by solving the direct problem. For example, Leon et al. [6] analyzed the consequences of a fire inside pyrotechnic stores to study effective prevention and protection measures in order to decrease explosion risk and prevent future accidents. Kraft et al. [7] developed dimensionless models to solve them and estimate safety distances in boiling liquid expanding vapor explosions. Zhai and Chen [8] created a model to estimate the damage on an island or reef under a missile warhead attack.

Another application of the direct problem is the evaluation of the consequences of an explosion. Sanchez-Monreal et al. [9] developed a simulation tool to evaluate the damage to people and structures using a simplified structural model and probability functions (Probit). Baraza et al. [10] conducted a multifactor analysis of the explosion of a lorry transporting ammonium nitrate due to a road accident to know all possible causes. Among other results, they estimated the mass of ammonium nitrate by using models to calculate the effects of the explosion with different masses and compare them with real ones.

This last paper shows another application of mathematical modeling of explosions: the determination of the causes based on the consequences. In numerous practical scenarios, the inverse of the direct problem arises: the process has already occurred, its outcomes are known, and the objective is to determine the underlying causes or initial conditions that led to it. By employing the system model, it becomes possible to estimate these initial conditions or model parameters through the resolution of what is referred to as the inverse problem. It involves determining the causes or system parameters from observed effects or data. The inverse problem consists of recovering unknown parameters, coefficients, or inputs from observations of the system response. This is often ill-posed: small measurement errors can cause large errors in the reconstruction [11–13]. The solution of the inverse problem has been used in many science and engineering fields to assess the inputs or parameters of a system or process [14–16].

Solving the inverse problem has also found applications in the analysis of different kinds of explosions [17–19]. Usually, the objective is to determine the parameters of the explosive sources from the consequences [20,21].

Finally, the novelty of this work lies in the proposal of an inverse protocol that enables a rapid calculation, based on the damage caused by an explosion, of the quantity of explosives that detonated. Furthermore, the study identifies the appropriate effects for the inverse problem—that is, those that would allow the mass of the explosive to be calculated whilst minimizing the error.

## 2. Mathematical models of direct and inverse problems

### *2.1. Direct problem*

Direct analysis of explosive phenomena constitutes a fundamental methodological framework in process safety engineering and loss prevention, as it enables a rigorous evaluation of the physical effects produced by the detonation of a known quantity of explosive material and their subsequent impact on civil structures, industrial equipment, and human populations. This analytical approach,

central to contemporary risk assessment practices, provides the basis for quantitatively estimating damage levels, establishing safety criteria, and designing structural protection or mitigation systems capable of withstanding highly transient dynamic loads. By characterizing the magnitude of the explosive source, the physical properties of the surrounding medium, the geometric configuration of the environment, and the vulnerability of exposed targets, the direct analysis approach generates predictive models that are critical for the prevention, control, and management of accidental or intentional explosive events.

Shock waves are discontinuities that propagate at supersonic velocities through compressible media, inducing abrupt and nonlinear changes in pressure, density, temperature, and particle velocity across the wavefront. The gradients that characterize the shock front represent localized regions of extreme thermodynamic transformation, typically idealized through the Rankine–Hugoniot relations, which describe the conservation of mass, momentum, and energy across the discontinuity. As illustrated schematically in Figure 1, the shock front delineates a near-instantaneous transition between pre- and post-shock states of the gas. Within the context of explosion analysis, shock waves acquire distinctive importance due to their ability to produce extreme overpressures, rapid impulse transfer, and complex reflection patterns that greatly influence structural response [22].

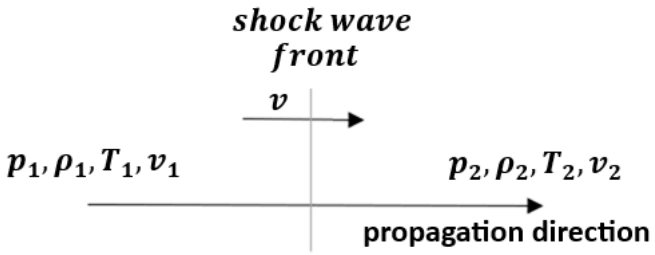


**Figure 1.** Shock wave from an explosion.

The behavior of shock waves is described by the conservation laws of fluid mechanics. The Rankine–Hugoniot equations express the conservation of mass, momentum, and energy across the discontinuity. For analytical simplicity, a one-dimensional stationary shock is assumed, meaning the shock front remains fixed in the reference system while the gas flows through it. Under the further assumption that the fluid behaves as an ideal gas, the governing relations are:

- Conservation of mass flux: the mass passing through the shock per unit area and time is identical on both sides.
- Conservation of momentum: the balance between pressure forces and momentum transport must be maintained.
- Conservation of energy: the sum of internal and kinetic energy is constant across the discontinuity.

With these considerations, the aforementioned equations are [23]:

$$\rho_1 u_1 = \rho_2 u_2, \quad \text{Conservation of mass flux,} \tag{1}$$

$$p_1 + \rho_1 u_1^2 = p_2 + \rho_2 u_2^2, \quad \text{Conservation of momentum,} \tag{2}$$

$$h_1 + \frac{1}{2}{u_1}^2 = h_2 + \frac{1}{2}{u_2}^2, \quad \text{Conservation of energy.} \tag{3}$$

The first equation ensures that the mass passing through the shock wave per unit time and area is the same on both sides of the discontinuity. The second expression represents the dynamic equilibrium

between the pressure forces and the transport of momentum. Finally, the third equation indicates that the total energy (internal plus kinetic) is conserved through the shock.
To solve the system, an additional relationship between the thermodynamic variables is required, which, in the case of an ideal gas, is as follows:

$$pv = RT. \tag{4}$$

If the analysis is extended to two or three dimensions, the equations become more complex, since velocity is no longer a scalar but a vector with components in different directions. In addition, shock waves can be oblique or curved, and additional partial derivative terms appear that represent momentum transport in cross directions. This requires the use of partial differential equations (PDEs) in coupled systems for mass, momentum, and energy.

For these reasons, one-dimensional treatment is a very useful first approximation for studying the phenomenon in a simplified way, but complete analysis in multiple dimensions requires more sophisticated numerical tools.

A very useful relationship in the study of the effects produced by explosions is Hopkinson's law, also known as the cubic root scaling law, which is empirical and widely used [24,25]. This law states that the effects generated by an explosion, such as shock wave pressure or damage range, do not depend directly on the mass of the explosive in a linear manner but are related to the distance from the detonation point and the cubic root of the explosive mass. This methodology, used for open detonations, has been widely used, and its results, provided theoretically, have been compared with experimental results [26–28]. The mathematical expression that summarizes this law is as follows:

$$z = \frac{r}{W^{1/3}}, \tag{5}$$

where Z is the scaled distance, r is the actual distance from the center of the explosion, and W is the mass of the explosive. This scaled distance has units of $(m/kg^{1/3})$ and is not a dimensionless quantity. Its main usefulness lies in the fact that it allows explosions of different magnitudes to be compared in a consistent manner. If two different explosions have the same Z value, then they are expected to produce similar effects, even if one uses more explosives and is measured at a greater distance. This is essential for extrapolating results from small-scale tests to large-scale real-world situations, such as in the design of explosion-resistant structures or in the planning of safety zones. The cubic root appears because the energy released by an explosion disperses in space, and the volume of impact grows with the cube of a characteristic distance. Therefore, by normalizing the distance by the cubic root of the explosive mass, a relative measure is obtained that allows us to predict how the effects vary with the scale of the explosion.

The TNT equivalent method is based on establishing the equivalence between the mass of any explosive substance and the mass of TNT using an equivalence factor (f), $W_{TNT} = f\,W$, obtaining the same results in both cases. The use of this method is supported by the large amount of information available in the literature on TNT explosions. In the direct method of explosion analysis using TNT equivalent mass, the two main parameters used to assess the effects on structures and people are maximum overpressure, p, and positive impulse, i, which are calculated from the scaled distance, Z. In addition to this scaled distance, empirical relationships or experimental tables [29] are used to estimate the magnitude of these parameters.

To translate physical blast parameters into meaningful risk metrics, a Probit methodology is applied [30–33], which allows these physical values to be translated into probabilities of damage to humans, as well as levels of damage to civil structures, facilitating risk assessment and decision-making for design or protection. Currently, the Probit methodology serves as a fundamental statistical

framework for quantifying risk in various technical fields, from pharmacological bioassays [34,35] and occupational risk prevention to industrial safety engineering [36–38], such as chemical inhalation [39], explosions [40–42], radiation, etc. [43,44].

This method uses equations of the following form:

$$Y = a + b\ \ Ln(F), \tag{6}$$

where Y is the Probit value, F is the relevant physical variable (e.g., overpressure in kPa or impulse in Pa·s), and a and b are empirical constants that depend on the type of damage. Then, the value of Y is converted into a probability, P, using the following statistical functions [30–33].

$$2.67 \leq Y \leq 3.59 \qquad P = 4.6439Y^4 - 54.598Y^3 + 245.52Y^2 - 495.03Y + 375.64, \tag{7}$$

$$3.59 \leq Y \leq 6.9 \qquad P = -3.25Y^3 + 48.76Y^2 - 206.60Y + 270.35, \tag{8}$$

$$6.9 \leq Y \leq 8.09 \qquad P = -0.832Y^4 + 26.502Y^3 - 317.57Y^2 + 1697.2Y - 3313.7. \tag{9}$$

This approach allows the estimation of human injury probabilities, structural damage levels, and equipment failure likelihoods. As such, the Probit method links deterministic shock physics with probabilistic risk assessment, supporting informed decision-making in engineering design and emergency planning.

Following the general Probit formulation introduced above, it becomes necessary to specify the quantitative relationships that link blast-wave parameters to the probability of injury or structural damage. While the Probit method provides a generic statistical framework—expressed in terms of a Probit variable Y and a physical descriptor F—the predictive capability of the methodology depends critically on the selection of appropriate empirical correlations. These correlations encapsulate experimental observations, accident data, and controlled testing results, translating the fundamental physics of shock-wave propagation with human and structural response. In this sense, the next set of equations represents a refinement of the Probit approach, adapted to specific damage mechanisms in both humans and buildings, and calibrated using TNT-equivalent scaling consistent with Hopkinson's law.

The introduction of these correlations is essential because different types of injury or structural failure are governed by distinct physical processes and thus require different functional dependencies on scaled distance, overpressure, impulse, or combined loading metrics. For instance, damages such as eardrum rupture or lung damage are dominated by peak overpressure and the corresponding rate of pressure rise, whereas skull fracture and whole-body impact involve more complex dynamics linked to inertia, acceleration, and the interaction of the human body with surrounding structures. Similarly, building damage cannot be characterized by a single blast parameter; instead, it often depends on a combination of local peak pressures, global impulses, reflected loads, and structural stiffness characteristics. Consequently, separate expressions for $F$ are required, each capturing the relevant scaling behavior and the sensitivity of the target (human or structure) to the imposed blast loads.

It is important to note that each correlation is applicable only within a specific numerical interval of F, which reflects the experimental domain from which the underlying data were obtained. Applying the equations outside these bounds would yield extrapolations of uncertain reliability and should therefore be avoided in rigorous risk assessments. The validity ranges listed alongside each expression are essential for ensuring that predictions remain consistent with the physical phenomena and empirical evidence. Moreover, because the correlation parameters are intrinsically linked to TNT-equivalent scaling, the analyst must ensure that the explosive event under consideration can reasonably be represented through TNT equivalence—an assumption generally valid for high-explosive detonations but less straightforward for fuel–air explosions.

The subsequent Eqs (10)–(24) organize these damage modes into two major categories—human damage and building damage—each containing several sub-mechanisms with their respective Probit formulations. Together, they constitute a comprehensive framework enabling the quantitative estimation of injury severity, fatality probability, structural impairment, and potential collapse. When integrated into the direct analysis of explosions, these correlations make it possible to translate physical blast parameters into probabilistic risk metrics, thereby bridging the gap between deterministic shock physics and decision-oriented safety engineering. The incorporation of these equations thus strengthens the analytical chain that connects source characterization, blast-wave propagation, scaled-distance formulation, empirical load estimation, and final risk quantification. Finally, it should be noted that Alonso et al. combined both methodologies, Probit and TNT equivalent, proposing the calculation of Probit number Y, which is related to the percentage of those affected, and a magnitude F, which implicitly includes overpressure and impulse [30–32].

### 2.1.1. Human damage

First, we present equations that represent different types of human injuries, such as eardrum rupture, death due to skull fracture, death due to whole body impact, and death due to lunge damage. The occurrence of one type of damage does not mean that other types of damage cannot occur: we can find a person who has died due to skull fracture but also suffered from whole body impact.

For eardrum rupture, the probit number Y, which is related to the percentage of people affected, is given by the following equation:

$$Y = 8.64 - 3.06\ \ lnF \qquad (1.20 \leq \mathrm{F} \leq 7.04), \tag{10}$$

where F is the scaled distance from the explosion's center in m/kg$^3$ (z) and the TNT equivalent mass in kilograms ($W_{TNT}$):

$$F = z/W_{TNT}^{1/3}. \tag{11}$$

Similarly, the equation for death due to skull fracture (probit number Y) is as follows:

$$Y = 57.15 - 8.49\ \ lnF \qquad (323.29 \leq \mathrm{F} \leq 612.14), \tag{12}$$

where

$$F = \left[\left(z/W_{TNT}^{1/3}\right)^{2.01} + (810.9z^{2.92}/W_{TNT}^{1.31})\right]. \tag{13}$$

The equation for death due to whole body impact is

$$Y = 17.28 - 2.44\ \ lnF \qquad (43.22 \leq \mathrm{F} \leq 398.50), \tag{14}$$

where

$$F = \left[\left(z/W_{TNT}^{1/3}\right)^{2.01} + (867.64z^{2.92}/W_{TNT}^{1.31})\right]. \tag{15}$$

Finally, the equation for death due to lung damage is

$$Y = 19.22 - 5.74\ \ lnF \qquad (6.95 \leq \mathrm{F} \leq 17.87), \tag{16}$$

where

$$F = \left[\left(z/W_{TNT}^{1/3}\right)^{2.41} + (99.34z^{0.91}/W_{TNT}^{0.64})\right]. \tag{17}$$

2.1.2. Building damage

Starting with minor building damage, the equation that defines the probit parameter Y and the F range valid for this equation is as follows:

$$Y = 5 - 0.26\ lnF \qquad (6.90\cdot10^{-6} \leq F \leq 7797.34), \tag{18}$$

where

$$F = \left(0.065z/W_{TNT}^{1/3}\right)^{7.84} + (0.51\ z/W_{TNT}^{0.7})^{4.55}\ ; \qquad \text{If } z/W_{TNT}^{1/3} \leq 10\ \ m/kg^{1/3} \tag{19}$$

and

$$F = \left(0.042z/W_{TNT}^{1/3}\right)^{4.52} + \ (0.35\ z/W_{TNT}^{0.65})^{5.3}\ ; \qquad \text{If } z/W_{TNT}^{1/3} > 10\ \ m/kg^{1/3}. \tag{20}$$

For major structural damage, the equation that defines the probit number Y is:

$$Y = 5 - 0.26\ lnF \qquad (6.90\cdot10^{-6} \leq F \leq 7797.34), \tag{21}$$

where

$$F = \ \left(0.126z/W_{TNT}^{1/3}\right)^{16.88} + (1.48\ z/W_{TNT}^{0.7})^{8.46}. \tag{22}$$

For building collapse, the probit number Y is given by

$$Y = 5 - 0.22\ lnF \qquad (7.95\cdot10^{-7} \leq F \leq 39771.63), \tag{23}$$

where

$$F = \left(0.19z/W_{TNT}^{1/3}\right)^{14.87} + (2.46\ z/W_{TNT}^{0.7})^{10.28}. \tag{24}$$

*2.2. Inverse problem*

The inverse problem in the study of explosion damage consists of determining the characteristics of the explosion based on the observed effects in the environment. Through the analysis of damage to structures, the aim is to estimate the quantity and location of the explosive. To solve this, iterations are performed comparing the results of simulations with the actual damage, adjusting the parameters until an acceptable match is achieved. This process is supported by physical and computational models. Its resolution is complex, as different scenarios can produce similar effects.

The relationships used in this work for the inverse problem, extracted from the equations of the direct problem, and which will be used later in the inverse problem protocol, are as follows:

2.2.1. Human damage

Eardrum rupture

$$F = e^{((Y-8.64)/-3.06)} \qquad (1.20 \leq F \leq 7.04), \tag{25}$$

$$W_{TNT} = (z/F)^3. \tag{26}$$

Death due to skull fracture

$$F = e^{((Y-57.15)/-8.49)} \qquad (323.29 \leq \mathrm{F} \leq 612.14), \tag{27}$$

$$W_{TNT} = ((z^{2.01}W_{TNT}^{0.64} + 810.9z^{2.92})/F)^{0.7634}. \tag{28}$$

Death due to whole body impact

$$F = e^{((Y-17.28)/-2.44)} \qquad (43.22 \leq \mathrm{F} \leq 398.50), \tag{29}$$

$$W_{TNT} = ((z^{2.01}W_{TNT}^{0.64} + 867.64z^{2.92})/F)^{0.7634}. \tag{30}$$

Death due to lung damage

$$F = e^{((Y-19.22)/-5.74)} \qquad (6.95 \leq \mathrm{F} \leq 17.87), \tag{31}$$

$$W_{TNT} = ((z^{2.41}W_{TNT}^{-0.1633} + 99.34z^{0.91})/F)^{1.5625}. \tag{32}$$

2.2.2. Building damage

Minor damage

$$F = e^{((Y-5)/-0.26)} \qquad (6.90\cdot10^{-6} \leq \mathrm{F} \leq 7797.34). \tag{33}$$

For $z/W_{TNT}^{1/3} \leq 10 \ \ m/kg^{1/3}$

$$W_{TNT} = ((4.93 \cdot 10^{-10}z^{7.84}W_{TNT}^{0.572} + 0.0467z^{4.55})/F)^{0.3139}. \tag{34}$$

For $z/W_{TNT}^{1/3} > 10 \ \ m/kg^{1/3}$

$$W_{TNT} = ((5.985 \cdot 10^{-7}z^{4.52}W_{TNT}^{1.938} + 0.00383z^{5.3})/F)^{0.2903}. \tag{35}$$

Major structural damage

$$F = e^{((Y-5)/-0.26)} \qquad (6.90\cdot10^{-6} \leq \mathrm{F} \leq 7797.34), \tag{36}$$

$$W_{TNT} = ((6.52 \cdot 10^{-16}z^{16.88}W_{TNT}^{0.296} + 27.569z^{8.46})/F)^{0.1689}. \tag{37}$$

Collapse

$$F = e^{((Y-5)/-0.22)} \qquad (7.95\cdot10^{-7} \leq \mathrm{F} \leq 39771.63), \tag{38}$$

$$W_{TNT} = ((1.884 \cdot 10^{-11}z^{14.87}W_{TNT}^{2.2393} + 10442.7z^{10.28})/F)^{0.13897}. \tag{39}$$

## 3. Protocol for the solution of the inverse problem

The inverse problem protocol consists of steps iii) to xi). In addition, steps i) and ii), which comprise the direct problem, are used to validate the proposed protocol, allowing the solution to the inverse problem to be compared with known data. This procedure has been applied in numerous studies [45–47].

The inverse problem protocol is validated using the results obtained from the direct problem simulation affected by a random error as input data. This allows the variables entered in the direct problem to be compared with the solution to the inverse problem. In addition, the protocol will also be applied to real cases. These steps are:

i) The direct problem for the detonation of explosives, pyrotechnics, or unstable substances of a determined mass of TNT equivalent ($W_{TNT}$) is simulated by defining the relationship between the

different effects (eardrum rupture, death due to skull fracture, death due to whole body impact, death due to lung damage, minor damage to buildings, major structural damage to buildings, and building collapse) and its distance.

ii) A random error ($\xi$ = 2%, 5%, 10%…, depending on the precision of the measurements of the real cases or of the experimental measurements) is applied to the percentage of each effect known ($\%_{i,\xi}$), for each distance ($\Delta z_\xi$), where i is ER for eardrum rupture, DSF for death due to skull fracture, DBI for death due to whole body impact, DLD for death due to lung damage, MD for minor damage to buildings, MSD for major structural damage to buildingsn and C for building collapse. An Excel® routine has been used to apply the random error as follows: value*(1 + (RAND() * ($\xi$*2/100) – ($\xi$/100))). We assume that these error-affected values are equivalent to those obtained by real effects or experimental measurements.

iii) The inverse protocol has to determine, on the one hand (first stage), the value of the equivalent TNT mass for each effect ($W_{TNT,i}$)—which can be obtained directly by Eqs (25) and (26) for the case of eardrum rupture and by iteration through Eqs (27)–(39) for the rest—and, on the other hand (second stage), to discriminate which values are correct in order to determine an average value. As will be discussed below, not all effects are suitable for the inverse problem, and it is advisable to use only eardrum rupture, minor damage to buildings, major structural damage to buildings, and building collapse, since they have a wide range of distribution of the percentage effect, i.e., the distance between the 100% and 0% percentage is large, so that the error in the result of the equivalent TNT mass when introducing a percentage affected by an error is smaller. However, for effects not included above, this distance is very short, going from 100% to 0% in just 5 m in some cases. Obviously, the 100% and 0% percentages should not be used, as the start of each of them is unknown, i.e., if the start of the 100% percentage is at 50 m, from 0 to 49 m they will also have a 100% percentage because the exposure to the explosion is greater.

iv) Set starting values for the mass of TNT equivalent ($W_{TNT,ini}$). For the initial value, if a relationship between distance and eardrum rupture percentage is known, it is calculated ($W_{TNT,ER}$), as it can be calculated directly without iteration, and an initial value is taken for all other effects ($W_{TNT,ini} = W_{TNT,ER}$). If not known, a random value is taken, e.g., 500 kg ($W_{TNT,ini}$ = 500 kg) for the calculation of the TNT equivalent mass of the other known effects.

v) From the simulation of Eqs (25)–(39), equivalent TNT mass is obtained for each of the known effects ($W_{TNT,i,j}$), where j is the iteration number to obtain the equivalent TNT mass value.

vi) Determine the value of the following functional $\left(\Psi_{W_{TNT}}^{i,j}\right)$ given by expression

$$\Psi_{W_{TNT}}^{i,j} = \sum_{j=1}^{j=N}\left(W_{TNT,i,j} - W_{TNT}^{*}\right)^2. \tag{40}$$

If $\Psi_{W_{TNT}}^{i,j} \geq 1$, go to step vii). If $\Psi_{W_{TNT}}^{i,j} < 1$, go to step viii).

vii) For the first simulation (j=1), then $W_{TNT}^{*} = W_{TNT,ini}$, where $W_{TNT}^{*}$ is the value of the mass of TNT equivalent in the right-hand side term of Eqs (27)–(39). For all other simulations (j>1) $W_{TNT}^{*} = W_{TNT}^{*} - 1$ if $W_{TNT,i,j} > W_{TNT}^{*}$, otherwise, $W_{TNT}^{*} = W_{TNT}^{*} + 1$. If the new value of $W_{TNT}^{*}$ is greater than zero ($W_{TNT}^{*} > 0$), go to step v). Otherwise, choose the value of $W_{TNT}^{*}$ for the minimum value of the functional $\Psi_{W_{TNT}}^{i,j}$ and then go to step viii). Note: A step size of ±1t is chosen for cases where the expected value is greater than this. For cases where a smaller value is expected, smaller steps such as 0.1t are used. This value can be adjusted depending on the level of precision required for the protocol.

viii) Retain the value of $W_{TNT,i}$ and go to step ix).

ix) In this step, the second stage begins. The mean value of the TNT equivalent mass ($W_{TNT,\,mean}$), Eq (41), and the confidence interval ($CI_{TNT}$) are calculated, Eq (42), with the 90% confidence interval being recommended as discussed below. For the calculation of the confidence interval, a normal distribution has been used [48], as the error distribution follows this type of distribution [49–51]. Go to step x).

$$W_{TNT,mean} = \frac{\sum_1^n W_{TNT,i}}{n}, \tag{41}$$

$$CI_{TNT} = W_{TNT,mean} \pm \alpha \frac{\sigma_{TNT}}{\sqrt{n}}, \tag{42}$$

where n is the number of known effects, α is the confidence level value, and $\sigma_{TNT}$ is the standard deviation. The value of α would be 1.96 for a 95% confidence level, 1.645 for a 90% confidence level, 1.44 for a 85% confidence level, and 1.282 for a 80% confidence level.

x) If the value of the TNT equivalent mass of any of the effects ($W_{TNT,i}$) lies outside the confidence interval ($CI_{TNT}$), both the mean and the confidence interval are recalculated without this value (go to step ix)); otherwise, go to step xi).

xi) Take as the value of the TNT equivalent mass ($W_{TNT}$) the mean value obtained ($W_{TNT,mean}$) with its confidence interval ($CI_{TNT}$).

xii) The following flowcharts (Figures 2 and 3) summarize the protocol for solving the direct and inverse problems.

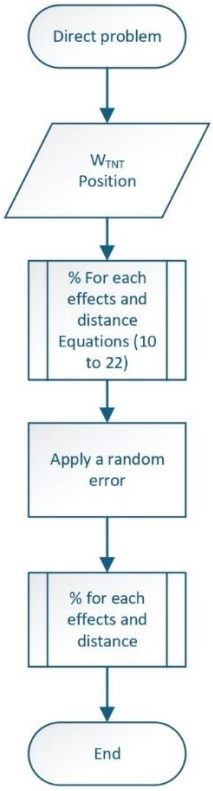


**Figure 2.** Flow diagram for the solution of the direct problem.

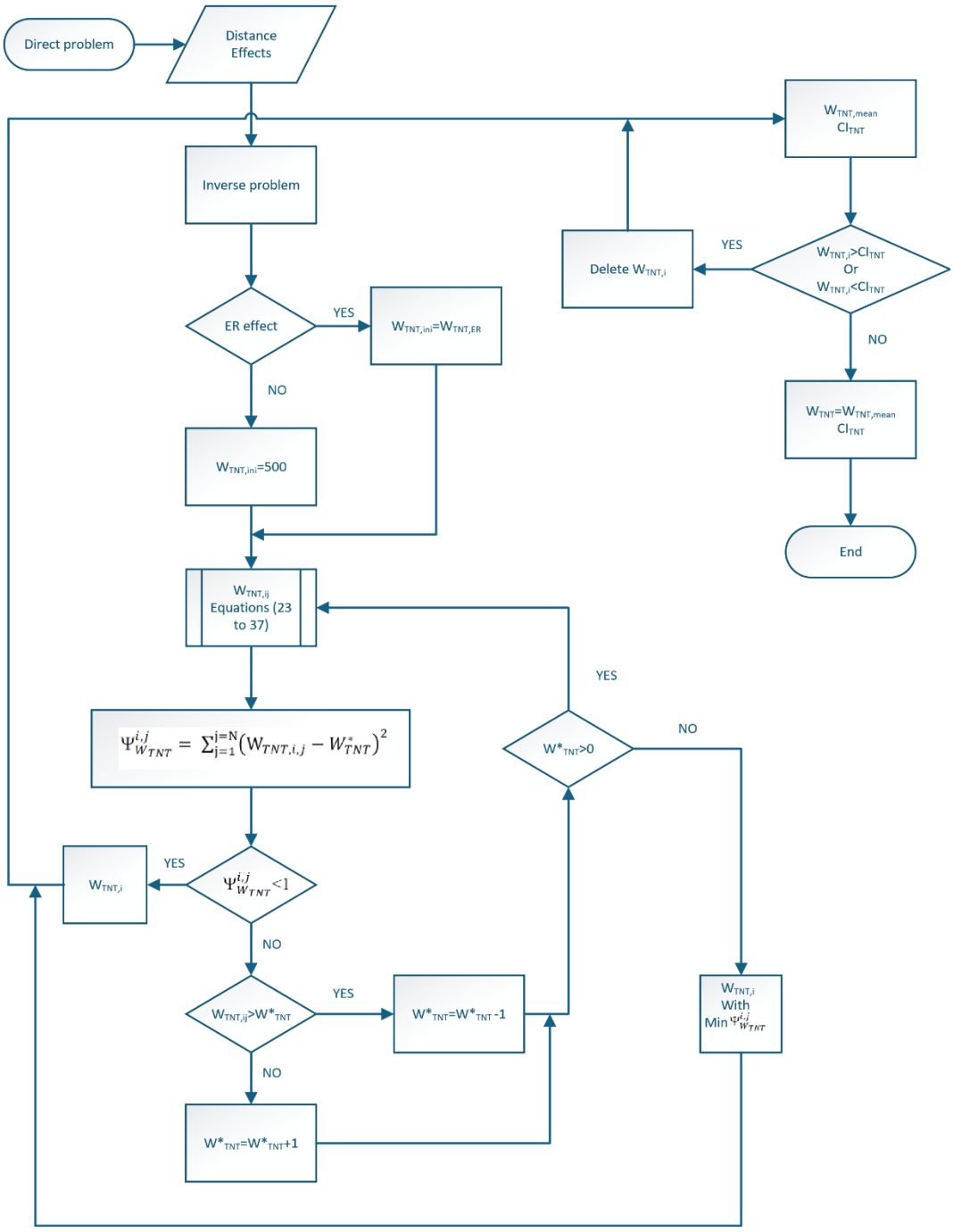


**Figure 3.** Flow diagram for the solution of the inverse problem.

The above steps (iii to xi) have been implemented in a MATLAB® work routine [52], which starts the calculation, checks the solutions, obtains the functionals, and enters the data for the new calculation, continuing until the final solution is obtained.

Verification of the results obtained using the inverse problem, with its inherent error, is straightforward: results are compared with the exact values, which were the input data in the direct problem. The error in the solution depends on the error applied to the input data.

## 4. Applications and verification

First, we will study which effects can be used for the inverse problem. To be useful, they must have an effect distribution that covers a wide distance. Thus, Table 1 shows distance distributions for each effect for different TNT equivalent masses using the direct problem. After the study, it can be concluded that for TNT equivalent mass values below 10 t, it is not advisable to use the death effects for the inverse problem, since they go from 100% to 0% in a matter of about 25 m, at best, making it challenging to determine their true value, which is subject to error. From this value, the effects of death due to whole body impact and death due to lung damage could be considered for the inverse problem. From 75 t, the effect of death due to skull fracture reaches a range of 25 m in the effects distribution and could be considered for the inverse problem. However, death effects should be avoided in the inverse protocol where possible, as even for the limits proposed above, the distance ranges are small. Regarding the eardrum rupture effect, although its distribution of affected percentages with respect to distance is greater, it is difficult to establish both the distance to the population and the percentage of those affected in real-life cases.

**Table 1.** Distribution of effects for different masses of equivalent TNT. ER: Eardrum rupture, DSF: Death due to skull fracture, DBI: Death due to whole body impact, DLD: Death due to lung damage, MD: Minor damage to buildings, MSD: Major structural damage to buildings; C: Building collapse.

| $W_{TNT}$ (t) | ER distance range (m) | DSF distance range (m) | DBI distance range (m) | DLD distance range (m) | MD distance range (m) | MSD distance range (m) | C distance range (m) |
|---|---|---|---|---|---|---|---|
| 0.1 | 6–33 | 5–8 | 3–7 | 1–4 | 3–310 | 3–49 | 3–29 |
| 1 | 14–71 | 16–21 | 8–17 | 7–16 | 17–1300 | 17–107 | 17–135 |
| 5 | 24–121 | 34–42 | 17–35 | 19–38 | 41–2840 | 41–240 | 41–190 |
| 10 | 31–160 | 46–57 | 24–48 | 28–52 | 52–3680 | 52–300 | 52–240 |
| 50 | 53–260 | 95–116 | 49–98 | 62–101 | 90–6370 | 90–500 | 90–400 |
| 75 | 61–300 | 114–139 | 59–118 | 74–119 | 103–7290 | 103–570 | 103–460 |

Finally, structural damage to buildings is more precise, both for the distance to the explosion, which is easy to determine using a GIS, and for determining the percentage of buildings affected for the three categories at a given distance.

In conclusion, if sufficient building damage data are available, they will be used in the inverse problem, and the equivalent TNT mass value obtained will be used by a direct problem to confirm the effects on the population. If sufficient data are not available, the eardrum rupture effect and the effects of fatalities on the TNT equivalent mass spectra specified above will also be used for the inverse problem. The minimum amount of data for the inverse problem that could be considered is four effects. Finally, probability data of 100% and 0% should be avoided, as the limit for this percentage is unknown. For example, if the threshold for 100% eardrum rupture is 35 m, this means that at 20 m there is also 100% eardrum rupture. The same is true for the 0% threshold.

Second, different cases will be performed by calculating the percentage effect for various distances and equivalent TNT masses. The results shown in Table 2 are the basis for the inverse problem.

**Table 2.** Case studies of the direct problem. ER: Eardrum rupture, DSF: Death due to skull fracture, DBI: Death due to whole body impact, DLD: Death due to lung damage, MD: Minor damage to buildings, MSD: Major structural damage to buildings, C: Building collapse.

| Case | $W_{TNT}$ (t) | Distance (m) | Effect (%) | | | | | | |
|---|---|---|---|---|---|---|---|---|---|
| | | | ER | MD | MSD | C | DSF | DBI | DLD |
| 1 | 0.1 | 50 | 0 | 56 | 0 | 0 | 0 | 0 | 0 |
| | | 100 | 0 | 23 | 0 | 0 | 0 | 0 | 0 |
| | | 150 | 0 | 0 | 0 | 0 | 0 | 0 | 0 |
| 2 | 1 | 50 | 9 | 98 | 88 | 48 | 0 | 0 | 0 |
| | | 100 | 0 | 82 | 15 | 2 | 0 | 0 | 0 |
| | | 150 | 0 | 66 | 0 | 0 | 0 | 0 | 0 |
| 3 | 5 | 50 | 63 | 100 | 100 | 98 | 0 | 0 | 0 |
| | | 100 | 4 | 98 | 92 | 37 | 0 | 0 | 0 |
| | | 150 | 0 | 88 | 34 | 5 | 0 | 0 | 0 |
| 4 | 10 | 50 | 86 | 100 | 100 | 100 | 73 | 0 | 2 |
| | | 100 | 15 | 100 | 100 | 65 | 0 | 0 | 0 |
| | | 150 | 1 | 97 | 71 | 19 | 0 | 0 | 0 |
| 5 | 50 | 50 | 100 | 100 | 100 | 100 | 100 | 100 | 100 |
| | | 100 | 71 | 100 | 100 | 99 | 91 | 0 | 1 |
| | | 150 | 27 | 100 | 100 | 79 | 0 | 0 | 0 |
| 6 | 75 | 50 | 100 | 100 | 100 | 100 | 100 | 100 | 100 |
| | | 100 | 84 | 100 | 100 | 100 | 100 | 11 | 32 |
| | | 150 | 41 | 100 | 100 | 91 | 0 | 0 | 0 |

Finally, in Table 3, the inverse problem is analyzed to determine which effects can be useful for the inverse problem protocol, using the results of the previous direct problem (Table 2). The analysis is applied to effects within ±10%, always in multiples of 5, since in real cases it is difficult to precisely know the percentage of effects at a given distance, as shown in case 13. In case 9, an effect well outside the range—the last one—is shown to evaluate the effectiveness of the inverse protocol. Cases 10–13 are real cases, with cases 10 and 11 being identical, except that the death effects are replaced by eardrum rupture effects, since, as concluded above, these effects are not useful for the inverse protocol [22].

Cases 12 and 13 are identical, with case 13 selected due to ambiguity in the data for this accident [22]. Cases 10 and 11 correspond to the Peterborough accident, involving a TNT-equivalent explosion of 800 kg. In this accident, at 10 m there was 100% eardrum rupture, 100% death due to skull fracture, 71% death due to body impact, and 35% death due to lung hemorrhage. At 20 m there was 90% eardrum rupture and 0% death effects. At 30 m there was 51% eardrum rupture and 0% death effects. At 50 m there was 6% eardrum rupture and 0% death effects. Finally, at 65 m, there was a 1% eardrum rupture and 0% death effects [31].

**Table 3.** Validation of the inverse protocol using the data of Table 2 affected by an error and real cases. ER: Eardrum rupture, DSF: Death due to skull fracture, DBI: Death due to whole body impact, DLD: Death due to lung damage, MD: Minor damage to buildings, MSD: Major structural damage to buildings, C: Building collapse. Confidence interval: 95% (α = 1.96), 90% (α = 1.645), 85% (α = 1.44), and 80% (α = 1. 282). ER: Relative error.

| Case | Effect | Effect | Effect | Effect | Effect | α | $W_{TNT}$ (t) | IC (t) | $W_{TNT,real}$ (t) | Er (%) |
|---|---|---|---|---|---|---|---|---|---|---|
| 7 | 1, 50 m, 15% | 2, 50 m, 95% | 2, 150 m, 70% | 3, 50 m, 85% | 4, 50 m, 55% | 1.96 | 1.033 | (0.825–1.241) | 1.00 | 3.30 |
| | | | | | | 1.645 | 1.033 | (0.858–1.208) | 1.00 | 3.30 |
| | | | | | | 1.44 | 0.927 | (0.927–0.927) | 1.00 | 7.30 |
| | | | | | | 1.282 | 0.927 | (0.927–0.927) | 1.00 | 7.30 |
| 8 | ER, 50 m, 65% | MD, 150 m, 90% | MSD, 150 m, 35% | C, 100 m, 40% | - | 1.96 | 5.177 | (5.155–5.200) | 5.00 | 3.54 |
| | | | | | | 1.645 | 5.177 | (5.158–5.196) | 5.00 | 3.54 |
| | | | | | | 1.44 | 5.177 | (5.161–5.194) | 5.00 | 3.54 |
| | | | | | | 1.282 | 5.457 | (5.457–5.457) | 5.00 | 9.14 |
| 9 | ER, 50 m, 90% | MSD, 150 m, 70% | C, 100 m, 65% | C, 150 m, 50% | - | 1.96 | 9.739 | (9.597–9.882) | 10.00 | 2.61 |
| | | | | | | 1.645 | 9.739 | (9.620–9.859) | 10.00 | 2.61 |
| | | | | | | 1.44 | 9.739 | (9.635–9.844) | 10.00 | 2.61 |
| | | | | | | 1.282 | 9.739 | (9.646–9.833) | 10.00 | 2.61 |
| 10 | ER, 20 m, 90% | ER, 30 m, 51% | ER, 50 m, 6% | DBI, 10 m, 71% | DLD, 10 m, 35% | 1.96 | 0.774 | (0.764–0.784) | 0.80 | 3.25 |
| | | | | | | 1.645 | 0.769 | (0.765–0.773) | 0.80 | 3.88 |
| | | | | | | 1.44 | 0.771 | (0.771–0.771) | 0.80 | 3.63 |
| | | | | | | 1.282 | 0.771 | (0.771–0.771) | 0.80 | 3.63 |
| 11 | ER, 20 m, 90% | ER, 30 m, 51% | ER, 50 m, 6% | ER, 65 m, 1% | - | 1.96 | 0.788 | (0.784–0.792) | 0.80 | 1.50 |
| | | | | | | 1.645 | 0.786 | (0.782–0.790) | 0.80 | 1.75 |
| | | | | | | 1.44 | 0.786 | (0.783–0.790) | 0.80 | 1.75 |
| | | | | | | 1.282 | 0.786 | (0.783–0.789) | 0.80 | 1.75 |
| 12 | C, 200 m, 86% | C, 300 m, 41% | MSD, 300 m, 93% | MD, 1000 m, 60% | MD, 2000 m, 29% | 1.96 | 147.5 | (145.4–149.6) | 150 | 1.67 |
| | | | | | | 1.645 | 148.5 | (147.4–149.6) | 150 | 1.00 |
| | | | | | | 1.44 | 146.7 | (145.0–148.3) | 150 | 2.20 |
| | | | | | | 1.282 | 146.7 | (145.2–148.1) | 150 | 2.20 |
| 13 | MSD, 430 m, 40% | MD, 720 m, 75% | MD, 1400 m, 50% | MD, 2050 m, 25% | | 1.96 | 134.3 | (113.1–155.5) | 150 | 10.5 |
| | | | | | | 1.645 | 143.8 | (128.7–158.9) | 150 | 4.1 |
| | | | | | | 1.44 | 143.8 | (130.6–156.9) | 150 | 4.1 |
| | | | | | | 1.282 | 143.8 | (132.0–155.5) | 150 | 4.1 |

Case 12 corresponds to the Toulouse accident with a TNT equivalent explosion of 150 t. In this accident, at 200 m there is 86% collapse, 95%–100% major structural damage, and 95%–100% between minor damage and no effect. At 300 m there is 41% collapse, 93% major structural damage, <98% minor damage, and <5% undamaged buildings. At 1000 m there is <5% collapse, <5% major structural damage, 60% minor damage, and 35%–40% undamaged buildings. Finally, at 2000 m there is <5% collapse, <5% major structural damage, 29% minor damage, and 66%–71% undamaged buildings. It is worth noting that the percentage of the minor damage effect includes both major structural damage and collapse; the percentage of the major structural damage effect includes collapse, since a building that has suffered major structural damage or collapse has also suffered minor damage,

and the same occurs with major structural damage and collapse [32]. Finally, case 13 also corresponds to the Toulouse accident with a TNT equivalent explosion of 150 t where the accident data has not been processed. In this accident, at 430 m there was "30%–50% destruction in incident facades, [and] some of the roofing components had been slightly torn away", which corresponds to a 30%–50% major structural damage. At 720 m, "one building had all the windows broken and the other approximately 50%", which corresponds to an average 75% minor damage. At 1400 m, "50% of the window panes [were] broken on the east/road façade", which corresponds to 50% minor damage. Finally, at 2050 m, "75% windows [were] broken at ground floor but no windows broken at first and second floor", which corresponds to an average of 25% minor damage [32].

Table 3 shows the validity of the inverse protocol by determining its optimal confidence interval. For all α values, relative error values below 11% are obtained, with the 90% interval ($\alpha = 1.645$) being selected, as it generally provides the lowest relative error and, in cases where it is higher, gives a value similar to the minimum. This α value results in relative errors of less than 4.5%. The α values of 1.44 and 1.282 are very restrictive, meaning that many values may fall outside the confidence interval (IC) and be eliminated. Because of this, and due to the number of decimal places selected, equal or similar confidence intervals (IC) can be obtained.

For case 9, the collapse value at 150 m was adjusted from 19%, as shown in case 4, to 50% to verify that the protocol can eliminate effect percentages that show significant deviation. Furthermore, the analysis of death effects confirms that they are not suitable for the protocol, as evidenced by the considerably reduced relative errors in cases 10 and 11. If these effects were to have large deviations, which is highly likely due to their range of distance distributions, the protocol would eliminate them, as shown in case 9, thus decreasing the number of data points used for the inverse protocol. Finally, comparing cases 12 and 13, which present treated and untreated data for a real accident, shows very similar results, with relative errors of 1% and 4.1%, respectively, for the 90% confidence interval.

## 5. Strengths and weaknesses

The application of the theoretical model to open detonation provides a standardized and robust framework for quantifying overpressure and impulse for different explosives. One of the main advantages of this approach is its predictive efficiency, which allows for rapid risk estimations and comparison of explosives using equivalent mass without the excessive computational burden of high-precision numerical simulations, finite-element simulations, or CFD [26]. However, these models have inherent weaknesses, particularly their tendency to oversimplify environmental variables and their reliance on static empirical constants that may not account for complex geometries or obstacles. Finally, it is worth noting that the methodology proposed in this work, although presented for theoretical models, can be adapted to numerical simulation methods, since what has been presented is a working algorithm.

## 6. Conclusions

In this work, an inverse problem protocol has been presented to estimate the explosive mass after an accidental explosion in which the effects, whether structural or on individuals, are known. As a new development, the most suitable effects for applying the inverse problem were identified, considering their distribution with respect to distance and the equivalent TNT mass. Effects related to mortality are not recommended for masses below 10 tons because the distance at which the effect occurs, encompassing 0 to 100% of the effect, is short, which introduces significant uncertainty in the estimation. Above 75 tons, the effect of death from skull fracture becomes somewhat relevant; however,

in general, lethal effects should be avoided in the inverse protocol, as even in these cases, the ranges remain limited and unreliable. However, the effect of a ruptured eardrum shows a wider distribution, but its practical application is complex due to the difficulty of determining both the exact distance to the population and the actual percentage of people affected. In contrast, structural damage to buildings proves to be the most accurate and reliable source for the inverse problem, thanks to the ease of determining distances using GIS systems and the ability to categorize damage at different levels.

Therefore, when sufficient data on building damage is available, this should form the basis of the inverse problem, complemented by the direct problem to validate the effects on individuals. If the data are insufficient, effects such as eardrum rupture and, in specific cases, mortality effects within the ranges specified above can be incorporated. Following the study, it can be estimated that the minimum acceptable dataset for applying the inverse protocol is at least four effects, avoiding extreme values of 0% and 100%, as their thresholds are uncertain.

Furthermore, analysis of the confidence interval suggests that using a 90% confidence interval minimizes the relative error, ensuring robust and accurate results for real-world applications. Furthermore, using the confidence interval allows filtering out excessively skewed data, ensuring that unreliable effects do not compromise the accuracy of the estimate. Thus, the protocol is designed to automatically discard such values, reinforcing its reliability even when the initial data quality varies.

Finally, the proposed method enables the mass of detonated explosives to be quickly identified using criteria derived from the study, at a low computational cost. A suggestion for future work would be to apply the inverse protocol to finite element simulations to improve accuracy and compare the results with theoretical equations.

## Author contributions

Juan Francisco Sánchez-Pérez: Conceptualization, methodology, software, validation, formal analysis, writing–original draft preparation, writing–review and editing; Manuel Conesa: Methodology, software, validation, formal analysis, writing–original draft preparation, writing–review and editing; José Jodar: Methodology, validation, formal analysis, writing–original draft preparation, writing–review and editing; Enrique Castro: Methodology, software, validation, formal analysis, writing–original draft preparation, writing–review and editing; Martina Fernández-García: Methodology, validation, formal analysis, writing–original draft preparation, writing–review and editing. All authors have read and agreed to the published version of the manuscript.

## Use of Generative-AI tools declaration

The authors declare they have not used Artificial Intelligence (AI) tools in the creation of this article.

## Conflict of interest

The authors declare no conflicts of interest.

## References

1. S. Sivaraman, S. Varadharajan, Investigative consequence analysis: A case study research of beirut explosion accident, *J. Loss Prevent. Proc.*, **69** (2021), 104387. https://doi.org/10.1016/j.jlp.2020.104387

2. G. Yu, Y. S. Duh, X. Yang, Y. Li, Y. Chen, Y. Li, et al., Holistic case study on the explosion of ammonium nitrate in Tianjin Port, *Sustainability*, **14** (2022). https://doi.org/10.3390/su14063429
3. X. Yang, Y. Li, Y. Chen, Y. Li, L. Dai, R. Feng, eat al., Case study on the catastrophic explosion of a chemical plant for production of m-phenylenediamine, *J. Loss Prevent. Proc.*, **67** (2020), 104232. https://doi.org/10.1016/j.jlp.2020.104232
4. R. P. Gilbert, J. Kajiwara, Y. S. Xu, *Direct and inverse problems of mathematical physics*, Boston: Springer, 2000. https://doi.org/10.1007/978-1-4757-3214-6
5. Y. Guo, T. Li, Fractional-order modeling and optimal control of a new online game addiction model based on real data, *Commun. Nonlinear Sci.*, **121** (2023), 107221. https://doi.org/10.1016/j.cnsns.2023.107221
6. D. Leon, B. Castells, I. Amez, J. Casin, J. G. Torrent, Experimental quantification of fire damage inside pyrotechnic stores, *Appl. Sci.-Basel*, **13** (2023), 6181. https://doi.org/10.3390/app13106181
7. R. A. Kraft, S. Orellano, P. L. Mores, N. J. Scenna, BLEVE: Safety distances estimation by simple models based on the Jakob number, *J. Loss Prevent. Proc.*, **83** (2023), 105069. https://doi.org/10.1016/j.jlp.2023.105069
8. C. Zhai, X. Chen, Damage assessment of the target area of the island/reef under the attack of missile warhead, *Def. Technol.*, **16** (2020), 18–28. https://doi.org/10.1016/j.dt.2019.06.022
9. J. S. Monreal, A. Cuadra, C. Huete, M. Vera, SimEx: A tool for the rapid evaluation of the effects of explosions, *Appl. Sci.-Basel*, **12** (2022), 9101. https://doi.org/10.3390/app12189101
10. X. Baraza, J. Gimenez, A. Pey, M. Rubiales, Lessons learned from the Barracas accident: Ammonium nitrate explosion during road transport, *Process Saf. Prog.*, **41** (2022), 519–530. https://doi.org/10.1002/prs.12396
11. M. Khosravi, M. Mohammadiun, H. Mohammadiun, M. H. D. Bonab, V. Parvaneh, Solving an inverse problem with four unknown boundary conditions in a lid-driven cavity with heated walls using the levenberg-marquardt method, *Appl. Eng. Sci.*, **23** (2025), 100245. https://doi.org/10.1016/j.apples.2025.100245
12. M. Baghban, Z. Shams, S. H. Pourhoseini, A sequential technique for solving the inverse problem associated with the assessment of time-dependent surface heat flux in a porous fin, *Int. J. Thermofluids*, **27** (2025), 101173. https://doi.org/10.1016/j.ijft.2025.101173
13. A. V. Trofimov, Adjoint state method in the block-parametric approach to the inverse problem analysis for elastic layered packages, *Mech. Res. Commun.*, **147** (2025), 104426. https://doi.org/10.1016/j.mechrescom.2025.104426
14. S. H. Rhie, E. Coatanéa, S. Lee, W. Jung, J. Lee, Resolving forward and inverse problems of rarefied gas heat transfer in an infrared detector cryochamber using physics-informed neural networks, *Appl. Therm. Eng.*, **277** (2025), 127104. https://doi.org/10.1016/j.applthermaleng.2025.127104
15. S. V. Khaustov, V. V. Pai, V. I. Lysak, S. V. Kuz'min, A. D. Kochkalov, The influence of the shock-compressed gas composition in the gap between metal plates on the processes occurring before contact point during explosion welding, *Int. J. Heat Mass Tran.*, **244** (2025), 126920. https://doi.org/10.1016/j.ijheatmasstransfer.2025.126920
16. F. Alhama, J. A. J. Valera, I. Alhama, Inverse problem protocol to estimate horizontal groundwater velocity from temperature–depth profiles in a 2D aquifer, *Appl. Sci.*, **14** (2024), 922. https://doi.org/10.3390/app14020922
17. J. F. S. Pérez, I. Alhama, Simultaneous determination of initial porosity and diffusivity of water-saturated reinforced concrete subject to chloride penetration by inverse problem, *Constr. Build. Mater.*, **259** (2020), 120412. https://doi.org/10.1016/j.conbuildmat.2020.120412

18. C. Yang, H. Zheng, X. Liu, X. Li, A novel data-analysis method for underwater explosion tests by inverse modeling, *Appl. Math. Model.*, **90** (2021), 1153–1169. https://doi.org/10.1016/j.apm.2020.10.030
19. J. F. Sánchez-Pérez, G. García-Ros, E. Castro, Simultaneous determination of the position, release time and mass release rate of an unknown gas emission source in short-term emissions by inverse problem, *Chem. Eng. J.*, **445** (2022), 136782. https://doi.org/10.1016/j.cej.2022.136782
20. X. Zhou, C. Bai, Y. Zhang, Z. Wang, Inverse analysis of explosives based on crater size, *Shock Waves*, **27** (2017), 27–35. https://doi.org/10.1007/s00193-016-0643-2
21. F. Hernandez, M. Abdel-Jawad, H. Hao, Simplified multiple equations' inverse problem of vented vessels subjected to internal gas explosions, *J. Loss Prevent. Proc.*, **35** (2015), 65–79. https://doi.org/10.1016/j.jlp.2015.03.007
22. S. Mannan, *Lees' loss prevention in the process industries*, 2012. https://doi.org/10.1016/C2009-0-24104-3
23. B. Lewis, G. V. Elbe, *Combustion, flames and explosions of gases*, Elsevier, 2012. https://doi.org/10.1016/C2009-0-21751-X
24. J. Manuel, B. Cadavid, *Vibraciones causadas por actividad humana: Caracterización, efectos y manejo en la Ingeniería Civil*, 2003.
25. F. D. Alonso, *Análisis de consecuencias y Zonas de Planificación para explosiones industriales accidentales (en el ámbito de las Directivas Seveso)*, Thesis, Universidad de Murcia, 2008.
26. H. Kwon, K. Tak, S. Maken, H. Kim, J. Park, I. Moon, Analysis of air blast effect for explosives in a large scale detonation, *Korean J. Chem. Eng.*, **34** (2017), 3048–3053. https://doi.org/10.1007/s11814-017-0227-6
27. L. Li, J. Chen, J. Liang, Z. Lai, Coupled ALE–Lagrangian analysis of pavement damage induced by buried natural gas pipeline explosions, *Infrastructures*, **11** (2025) 10. https://doi.org/10.3390/infrastructures11010010
28. S. H. Lee, B. Y. Choi, H. S. Kim, Probabilistic blast load for performance-based blast resistant design of building structures in petrochemical facilities, *J. Build. Eng.*, **98** (2024), 111313. https://doi.org/10.1016/j.jobe.2024.111313
29. T. N. O. Book, Methods for the determination of possible damage, *Rep. CPR E*, **16** (1989), 28.
30. F. D. Alonso, E. G. Ferradás, J. F. S. Pérez, A. M. Aznar, J. R. Gimeno, J. M. Alonso, Characteristic overpressure-impulse-distance curves for the detonation of explosives, pyrotechnics or unstable substances, *J. Loss Prevent. Proc.*, **19** (2006), 724–728. https://doi.org/10.1016/j.jlp.2006.06.001
31. F. D. Alonso, E. G. Ferradás, J. F. S. Pérez, A. M. Aznar, J. R. Gimeno, J. M. Alonso, Consequence analysis by means of characteristic curves to determine the damage to humans from the detonation of explosive substances as a function of TNT equivalence, *J. Loss Prevent. Proc.*, **20** (2007), 187–193. https://doi.org/10.1016/j.jlp.2007.03.003
32. F. D. Alonso, E. G. Ferradás, M. D. Miñarro, A. M. Aznar, J. R. Gimeno, J. F. S. Pérez, Consequence analysis by means of characteristic curves to determine the damage to buildings from the detonation of explosive substances as a function of TNT equivalence, *J. Loss Prevent. Proc.*, **21** (2008), 74–81. https://doi.org/10.1016/j.jlp.2007.08.002
33. J. F. S. Pérez, B. C. Jimenez, E. C. Rodriguez, M. Cánovas, M. Conesa, Characterization of workers or population percentage affected by low-back pain (LPB), sciatica and herniated disc due to whole-body vibrations (WBV), *Heliyon*, **10** (2024), e31768. https://doi.org/10.1016/j.heliyon.2024.e31768

34. T. Ara, H. Kitamura, Y. C. Hung, K. I. Uchida, Construction and evaluation of a statistical model for a probit method simulator in pharmacological education, *Appl. Biosci.*, **4** (2025), 50. https://doi.org/10.3390/applbiosci4040050
35. A. A. Farfalla, C. Beseler, C. Achutan, R. Rautiainen, Coexposure to solvents and noise as a risk factor for hearing loss in agricultural workers, *J. Occup. Environ. Med.*, **64** (2022), 754–760. https://doi.org/10.1097/JOM.0000000000002571
36. Y. M. Kim, Y. Son, W. Kim, B. Jin, M. H. Yun, Classification of children's sitting postures using machine learning algorithms, *Appl. Sci.*, **8** (2018), 1280. https://doi.org/10.3390/app8081280
37. A. Amira, F. Innal, Risk assessment of industrial domino effects using stochastic Petri nets, *Int. J. Saf. Secur. Eng.*, **15** (2025), 150814. https://doi.org/10.18280/ijsse.150814
38. M. Su, L. Wei, S. Zhou, G. Yang, R. Wang, Y. Duo, et al., Study on dynamic probability and quantitative risk calculation method of domino accident in pool fire in chemical storage Tank area, *Int. J. Env. Res. Pub. He.*, **19** (2022), 16483. https://doi.org/10.3390/ijerph192416483
39. M. M. W. M. Ruijten, J. H. E. Arts, P. J. Boogaard, P. M. J. Bos, H. Muijser, A. Wijbenga, Method for derivation of probit functions for acute inhalation toxicity, *National Inst. Pub. He. Environ.*, 2015.
40. M. El-Harbawi, Fire and explosion risks and consequences in electrical substations—A transformer case study, *ASME Open J. Eng.*, **1** (2022), 014501. https://doi.org/10.1115/1.4054143
41. P. Russo, A. de Marco, F. Parisi, Assessment of the damage from hydrogen pipeline explosions on people and buildings, *Energies*, **13** (2020), 5051. https://doi.org/10.3390/en13195051
42. M. Jiang, Y. Yang, J. Bian, M. Fang, V. Cozzani, G. Reniers, et al., Explosion induced domino effect assessment in the process industries: A machine learning approach to improve probit models, *J. Loss Prevent. Proc.*, **98** (2025), 105714. https://doi.org/10.1016/j.jlp.2025.105714
43. M. Abouelouafa, H. El-Ossmani, Y. Bakri, S. Omari, A. Mbarki, Thermal radiation impact on cellular viability: Comparative modeling of tolerable and lethal distances using probit methods, *Perinat. J.*, **34** (2026), 1113–1123. https://doi.org/10.57239/prn.26.034100112
44. J. Zhou, G. Reniers, V. Cozzani, Improved probit models to assess equipment failure caused by domino effect accounting for dynamic and synergistic effects of multiple fires, *Process Saf. Environ.*, **154** (2021), 306–314. https://doi.org/10.1016/j.psep.2021.08.020
45. G. G. Ros, I. Alhama, Method to determine the constitutive permeability parameters of non-linear consolidation models by means of the oedometer test, *Mathematics*, **8** (2020), 1–19. https://doi.org/10.3390/math8122237
46. J. F. S. Pérez, I. Alhama, Simultaneous determination of initial porosity and diffusivity of water-saturated reinforced concrete subject to chloride penetration by inverse problem, *Constr. Build. Mater.*, **259** (2020), 120412. https://doi.org/10.1016/j.conbuildmat.2020.120412
47. J. Zueco, F. Alhama, Inverse estimation of temperature dependent emissivity of solid metals, *J. Quant. Spectrosc. Ra.*, **101** (2006), 73–86. https://doi.org/10.1016/j.jqsrt.2005.11.005
48. D. S. Shafer, Z. Zhang, *Introductory statistics*, LibreTexts, 2024. Available from: https://LibreTexts.org.
49. D. S. Shafer, Z. Zhang, Small sample estimation of a population mean, Introductory Statistics, LibreTexts, 2024. Available from: https://stats.libretexts.org/Bookshelves/Introductory_Statistics/Introductory_Statistics_.
50. STAT 462, *Chapter 6.3–Tests for error normality*, Applied Regression Analysis, 2025. Available from: https://online.stat.psu.edu/stat462/.
51. C. Croarkin, P. Tobias, NIST/SEMATECH e-handbook of statistical methods, **1** (2014). https://doi.org/doi.org/10.18434/M32189

52. The MathWorks, Inc. Matlab, MATLAB, 2022. Available from: https://es.mathworks.com/products/matlab.html.